

# The Tubulin Deglutamylase CCPP-1 Regulates the Function and Stability of Sensory Cilia in *C. elegans*

Robert O'Hagan,<sup>1</sup> Brian P. Piasecki,<sup>2</sup> Malan Silva,<sup>1</sup> Prasad Phirke,<sup>2</sup> Ken C.Q. Nguyen,<sup>3</sup> David H. Hall,<sup>3</sup> Peter Swoboda,<sup>2</sup> and Maureen M. Barr<sup>1,\*</sup>

<sup>1</sup>Department of Genetics, Rutgers, The State University of New Jersey, Piscataway, NJ 08854, USA

<sup>2</sup>Department of Biosciences and Nutrition, Center for Biosciences at NOVUM, Karolinska Institute, Hälsovägen 7, S-141 83 Huddinge, Sweden

<sup>3</sup>Center for *C. elegans* Anatomy, Albert Einstein College of Medicine, 1410 Pelham Parkway, Bronx, NY 10461, USA

## Summary

**Background:** Posttranslational modifications (PTMs) such as acetylation, detyrosination, and polyglutamylation have long been considered markers of stable microtubules and have recently been proposed to guide molecular motors to specific subcellular destinations. Microtubules can be deglutamylated by the cytosolic carboxypeptidase CCP1. Loss of CCP1 in mice causes cerebellar Purkinje cell degeneration. Cilia, which are conserved organelles that play important diverse roles in animal development and sensation, contain axonemes comprising microtubules that are especially prone to PTMs.

**Results:** Here, we report that a CCP1 homolog, CCPP-1, regulates the ciliary localization of the kinesin-3 KLP-6 and the polycystin PKD-2 in male-specific sensory neurons in *C. elegans*. In male-specific CEM (cephalic sensilla, male) cilia, *ccpp-1* also controls the velocity of the kinesin-2 OSM-3/KIF17 without affecting the transport of kinesin-II cargo. In the core ciliated nervous system of both males and hermaphrodites, loss of *ccpp-1* causes progressive defects in amphid and phasmid sensory cilia, suggesting that CCPP-1 activity is required for ciliary maintenance but not ciliogenesis. Affected cilia exhibit defective B-tubules. Loss of TTL-4, a polyglutamylating enzyme of the tubulin tyrosine ligase-like family, suppresses progressive ciliary defects in *ccpp-1* mutants.

**Conclusions:** Our studies suggest that CCPP-1 acts as a tubulin deglutamylase that regulates the localization and velocity of kinesin motors and the structural integrity of microtubules in sensory cilia of a multicellular, living animal. We propose that the neuronal degeneration caused by loss of CCP1 in mammals may represent a novel ciliopathy in which cilia are formed but not maintained, depriving the cell of cilia-based signal transduction.

## Introduction

Cilia are microtubule (MT)-based organelles that are present on most nondividing eukaryotic cells and are essential for vision, olfaction, hearing, and embryonic development [1]. Ciliary axonemes typically have a “9 + 2” or “9 + 0” MT

formation (nine outer doublets with two inner singlets, or nine outer doublets with zero inner singlets), but variations do occur [1].

All motile and nonmotile eukaryotic cilia are built by a process called IFT (intraflagellar transport) [2]. Anterograde IFT is driven by heterotrimeric kinesin-II motors that transport IFT-A and IFT-B complexes [2]. This basic IFT machinery can be accompanied by other accessory motors. *C. elegans* amphid channel cilia are built by the cooperative action of two kinesin-2 motors—homodimeric kinesin-2 OSM-3 and heterotrimeric kinesin-II, comprising KLP-11, KLP-20, and KAP-1 [2, 3]. In *C. elegans* male-specific CEM (cephalic sensilla, male) cilia, the kinesin-3 KLP-6 moves independently of the IFT kinesin-2 motors and reduces the velocity of OSM-3 [4]. In humans, mutations that affect cilia formation or function can cause genetic diseases called ciliopathies that display pleiotropic defects, including cystic kidneys, retinal photoreceptor degeneration, anosmia, and sperm immotility [2].

Ciliary axonemal MTs are subject to posttranslational modifications (PTMs). PTMs are considered to be markers of stable microtubules and can regulate the activities of kinesin and dynein motors [5–8]. For example, localization of the kinesin-3 KIF1A to axons and dendrites is regulated by the level of MT polyglutamylolation [9]. At present, our understanding of the physiological relevance of tubulin PTMs is very limited.

We report here several ciliary defects arising from a mutation in the gene *ccpp-1*, which encodes a cytosolic carboxypeptidase tubulin modifying enzyme. The *ccpp-1(my22)* mutant was isolated in a genetic screen for defective ciliary localization of PKD-2::GFP, a functional fluorescently tagged transient receptor potential (TRP) polycystin ion channel [10]. The murine homolog CCP1 (also called Nna1 or AGTPBP1) is a deglutamylating enzyme that reduces the polyglutamylolation that is added as a side chain to glutamate residues in the C terminus of tubulin [11]. CCP1 also removes the penultimate amino acid, a glutamate, encoded in the primary sequence of tubulin to produce  $\Delta 2$ -tubulin [11].

*C. elegans ccpp-1* mutants also displayed defects in localization of the kinesin-3 KLP-6 and abnormal motility of OSM-3/KIF17 in male-specific cilia required for mating behavior. In amphid and phasmid neurons, loss of CCPP-1 function caused progressive ciliary dye-filling (Dyf) defects, suggesting that ciliary structure is not maintained. The progressive Dyf defect in *ccpp-1* mutants was dependent on TTL-4, a polyglutamylase of the tubulin tyrosine ligase-like family. *ccpp-1* animals also displayed cell-specific defects in ciliary polyglutamylolation signals. Our results provide the first demonstration that CCPP-1 regulates the function and stability of sensory cilia. Loss of function of CCP1 in *pcd* mice causes progressive degeneration of cerebellar Purkinje neurons, thalamic neurons, retinal photoreceptors, and olfactory mitral neurons, as well as sperm immotility [12, 13], phenotypes that are reminiscent of human ciliopathies. We propose that CCPP-1 affects the structure and stability of ciliary MTs, the function of ciliary kinesins, and ciliary localization of their cargoes, by regulating the polyglutamylolation state of ciliary MTs.

\*Correspondence: [barr@biology.rutgers.edu](mailto:barr@biology.rutgers.edu)

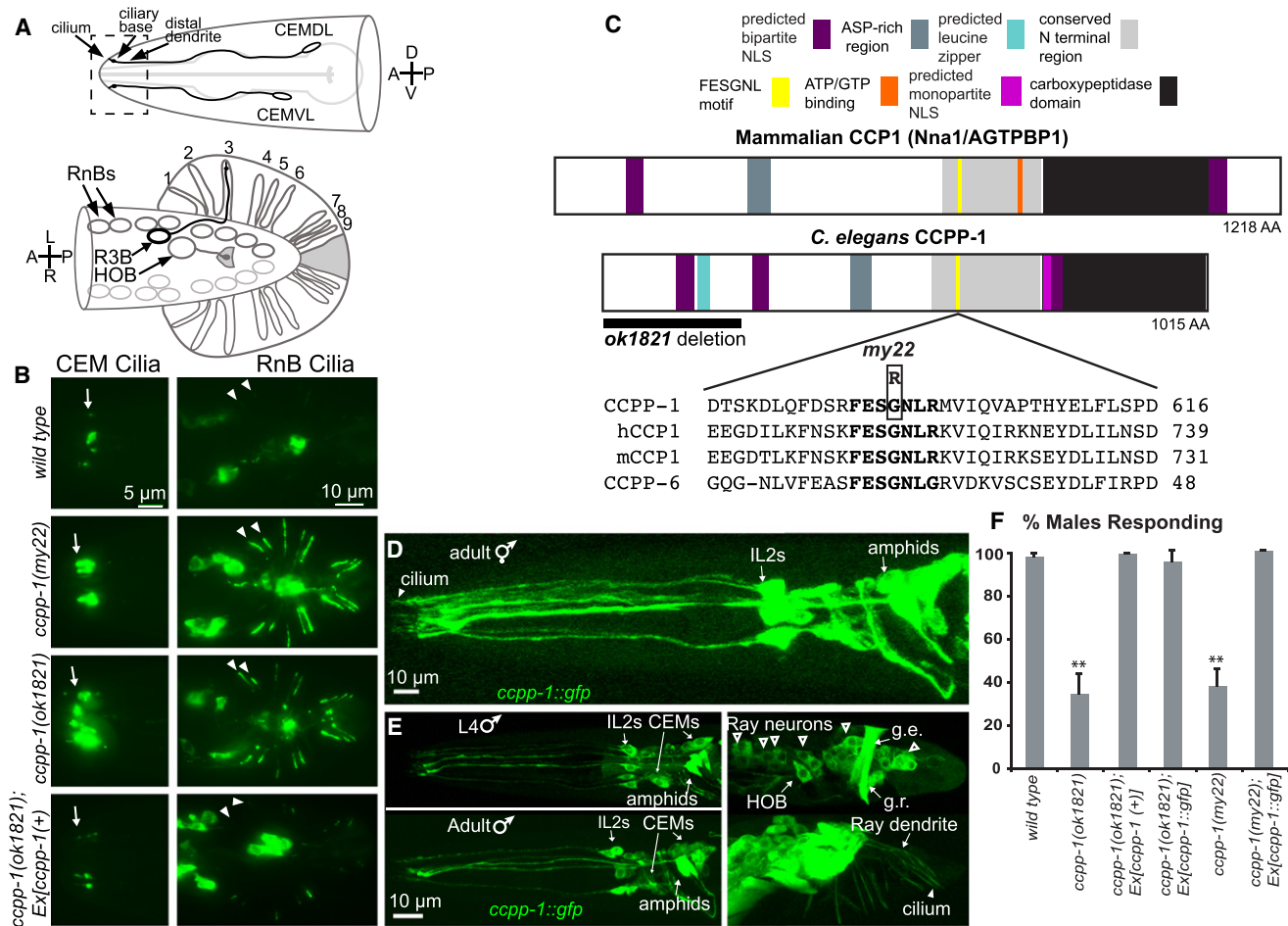


Figure 1. CCPP-1 Is Required for PKD-2 Localization and Is Expressed in the Ciliated Sensory Nervous System

(A) Diagram of the male-specific CEM neurons in the head and hook B-type (HOB) and RnB (ray B-type, where n = 1–9, excluding 6) neurons in the tail. Box illustrates the region of CEM (cephalic sensilla, male) cilia and distal dendrites shown in the epifluorescent images. In the ventral-up cartoon of the male tail, the RnBs innervate the tail rays; R3B dendrite is shown as an example.

(B) In wild-type males, PKD-2::GFP faintly illuminated cilia of the CEM neurons, the HOB cilium, and the cilia of the RnB neurons. *ccpp-1(my22)* and *ccpp-1(ok1821)* mutants exhibit the Cil phenotype. Arrows point to CEM cilia; arrowheads point to R1B and R2B cilia. Expression of genomic *ccpp-1* rescued the Cil phenotype of *ccpp-1(ok1821)*.

(C) CCPP-1 contains several conserved regions, including a zinc carboxypeptidase domain, an aspartic-acid rich domain, a conserved “NT” region (N-terminal to the carboxypeptidase domain; [12]), and predicted NLS (nuclear localization signal; [36]). CCPP-1 also contains a predicted leucine zipper near the N terminus (ScanProsit [37]). The *my22* lesion affects the conserved sequence FESGNL in the NT region of CCPP-1.

(D) In adult hermaphrodites, CCPP-1::GFP was expressed in amphid and IL2 core ciliated sensory neurons. A cilium containing CCPP-1::GFP is indicated.

(E) Confocal projections of CCPP-1::GFP expression in males. Top (L4): CCPP-1::GFP was expressed in (left) amphid, IL2, and CEM neurons and (right) male tail ray and HOB neuronal cell bodies (empty arrowheads). Gubernacular erector (g.e.) and retractor (g.r.) muscles are indicated. Bottom (1-day-old adult): CCPP-1::GFP localization in ray neuron dendrites (arrow) and a cilium (arrowhead) is shown.

(F) *ccpp-1* mutants are defective in response behavior. Number of trials and number of males for each genotype was as follows: wild-type, seven trials, n = 70 males; *ok1821*, six trials, n = 60; *ok1821;Ex[ccpp-1(+)]*, three trials, n = 29; *ok1821;Ex[ccpp-1::gfp]*, three trials, n = 24; *my22*, four trials, n = 40; *my22;Ex[ccpp-1::gfp]*, five trials, n = 39. Error bars indicate standard error of the mean (SEM); \*\* indicates that *ccpp-1* mutants were statistically different ( $p < 10^{-4}$ , analysis of variance [ANOVA]/Tukey HSD test) from mutants expressing *ccpp-1* transgenes, which were similar to wild-type. See also Figure S1.

## Results

### *my22* and *ok1821* Are Alleles of *ccpp-1*, which Is Required for Proper Localization of PKD-2::GFP

We isolated the *my22* allele in a screen for ciliary PKD-2::GFP localization defective mutants [10]. PKD-2::GFP localizes to cilia located on the distal dendrites of CEMs, RnBs (ray B-type, where n = 1–9, excluding 6), and HOB (hook B-type) male-specific neurons (Figures 1A and 1B) [14]. In *my22* males, excessive PKD-2::GFP accumulates in cilia and distal

dendrites (hereafter referred to as the Cil phenotype; Figure 1B) [10].

We mapped *my22* to a region between +0.39 and +0.5 cM on chromosome I. The Cil phenotype in *my22* mutants was rescued by germline injection of fosmid WRM0627dB11, which contains full genomic sequence of seven genes, of which only the *ccpp-1(ok1821)* mutant failed to complement *my22* for the Cil phenotype. *ccpp-1(ok1821)* males also displayed the Cil phenotype, which was rescued by a genomic *ccpp-1(+)* transgene (Figure 1B). We conclude that both

### **C. elegans CCPP-1 Regulates Ciliary Stability**

3

*my22* and *ok1821* are recessive alleles of a single gene, *ccpp-1*.

#### **The *my22* Molecular Lesion Affects a Conserved Domain in CCPP-1**

The *my22* lesion is a G-A transition encoding a G596R amino acid substitution (Figure 1C) in the conserved sequence FESGNL (Figure 1C). The *ccpp-1(ok1821)* mutation encodes a deletion that removes putative 5' regulatory sequences as well as the first five exons of the *ccpp-1* locus and may be a genetic null (Figure 1C). BLAST (basic local alignment search tool; [15]) searches of *C. elegans* CCPP-1 against human sequences revealed several conserved domains, including a zinc carboxypeptidase domain [16] (Figure 1C) and showed that residues 536–1,015 are 43% identical to human CCP1 residues 573–1,122. Hence, *ccpp-1* encodes an evolutionarily conserved protein.

#### **CCPP-1::GFP Is Expressed in the Ciliated Sensory Nervous System**

We analyzed expression and localization of a *ccpp-1::gfp* translational reporter. CCPP-1::GFP was neuronally expressed in developing embryos (not shown) through adulthood in amphid and IL2 ciliated sensory neurons of the core nervous system, which males and hermaphrodites have in common (Figures 1D and 1E). In the male-specific nervous system, CCPP-1::GFP was coexpressed with *pkd-2* in CEM head neurons and the RnB and HOB neurons in the tail (Figure 1E). CCPP-1::GFP was also expressed in some unidentified neurons and the gubernacular erector and retractor muscles in the male tail (Figure 1E). CCPP-1::GFP was localized diffusely throughout neurons, including cilia, but excluded from the nucleus.

To determine whether CCPP-1::GFP was functional, we assayed the mating behavior of transgenic males. *ccpp-1* mutant males are defective in the response substep of mating (Figure 1F) [10], in which males sense contact with and begin scanning the body of a potential hermaphrodite mate [17]. Response behavior requires the ray neurons [14, 18]. Whereas 99% ± 1% of wild-type males (seven trials, n = 70 animals total assayed) responded to hermaphrodite mates within 4 min, only 38% ± 8% of *ccpp-1(my22)* (four trials, n = 40) and 35% ± 9% of *ccpp-1(ok1821)* males responded (six trials, n = 60) (Figure 1F). Genomic *ccpp-1(+)* and *ccpp-1::gfp* transgenes rescued the response defect in *ccpp-1* mutant males (Figure 1F). Hence, the CCPP-1::GFP translational fusion protein was functional in RnB neurons.

#### ***ccpp-1* Mutants Exhibit a Progressive Defect in Ciliary Structure**

We performed dye-filling assays to assess the structural integrity of cilia in the amphid and phasmid sensillae of *ccpp-1* mutants [19]. Wild-type amphid and phasmid ciliated sensory neurons took up a lipophilic fluorescent dye through environmentally exposed ciliated endings (Figures 2A and 2B [19]). Mutants with ciliary structure defects, such as *osm-3(p802)* and the IFT-B polypeptide mutant *che-13(e1805)*, exhibit the Dyf phenotype at all developmental stages [19]. *ccpp-1(ok1821)* hermaphrodites displayed an age-dependent Dyf defect (Figures 2A and 2B). In young *ccpp-1* larvae (L1 or L2), amphid dye-uptake appeared nearly normal (Figure 2B), whereas L4 larvae and young adults showed a severe Dyf phenotype in ciliated sensory neurons in both the amphid and phasmid sensillae. Older adults displayed the most severe

Dyf phenotype. *ccpp-1(my22)* hermaphrodites displayed a similar, but less penetrant, age-dependent Dyf defect (Figure 2B), consistent with *ok1821* being a loss-of-function and *my22* being a reduction-of-function allele. The Dyf phenotype in *ccpp-1(ok1821)* animals at all ages was rescued by a *ccpp-1(+)* transgene (Figure 2B).

*C. elegans* relies on ciliated sensory neurons of the amphid sensilla to detect and avoid high osmolarity [20]. Cilium structure mutants, such as *che-13(e1805)*, are osmotic avoidance defective (the Osm phenotype) at all developmental stages (Figure 2C) [19, 20]. *ccpp-1* mutants exhibited progressive Osm defects that mirrored the progressive Dyf phenotype (Figure 2C). *ccpp-1(ok1821)* L1 and L2 larvae were slightly defective (avoidance index, or a.i., of  $0.80 \pm 0.06$ ;  $p < 0.0001$  versus  $1.0 \pm 0$  for wild-type; Figure 2C), but this defect became more severe with age (a.i. =  $0.23 \pm 0.01$  of 1- to 2-day-old adults;  $p < 0.0001$  versus  $0.99 \pm 0.04$  for wild-type; Figure 2C). As adults, *ccpp-1(my22)* mutants were also partially defective in osmotic avoidance behavior (Figure 2D). In all cases, the Osm phenotype of *ccpp-1* mutants was fully rescued by the *ccpp-1::gfp* transgene (Figure 2D). Based on the results of dye-filling and osmotic avoidance assays, which reflect the structure and function of amphid cilia, we propose that *ccpp-1* mutants are capable of forming but not maintaining sensory cilia.

#### ***ccpp-1* Mutants Display Ciliary Ultrastructural Defects Including B-Tubule Defects, Disorganization of MTs, and Ciliary Fragmentation**

To examine the ultrastructure of the CEM and amphid cilia, we used transmission electron microscopy (TEM) and electron tomography of fixed age-matched young adult males. Wild-type CEM cilia typically contained approximately 20 singlet MTs that were distributed spatially, with many singlets closely apposed to the membrane, when viewed in cross-section (Figure 3A; Table 1). CEM cilia in a *ccpp-1(ok1821)* male contained only 16 MT singlets on average, and those that remained were disorganized, residing on average four times farther from the membrane than in wild-type (Figure 3A; Table 1). The average diameter of *ccpp-1(ok1821)* CEM cilia was 66% larger than wild-type (Figure 3A; Table 1).

In wild-type males, the amphid channel middle segment region contained ten cilia, which each contained on average eight visible outer microtubule doublets (Figure 3B; Table 1). In a *ccpp-1(ok1821)* male, the amphid channel middle segment region contained an average of only eight intact cilia that had on average two outer doublets and few singlets, which appeared disorganized (Figure 3B; Table 1). Some of the singlets appeared to have attached remnants of B-tubules. Some missing cilia may have fragmented (Figure 3B; Table 1). Hence, CCPP-1 function is important for ciliary integrity as well as MT architecture.

#### **CCPP-1 Regulates Polyglutamylolation in Sensory Cilia**

Murine CCP1 removes the penultimate amino acid, a glutamate, of the primary sequence of  $\alpha$ -tubulin and shortens side chains of glutamates (polyglutamylolation) added to the C terminus of  $\alpha$ - and  $\beta$ -tubulins in stable microtubules [11]. CCPP-6 was reported to reduce polyglutamylolation in *C. elegans* sensory cilia [21].

If *ccpp-1* Cil and Dyf defects were caused by excessive glutamylolation of ciliary MTs, loss of a polyglutamylase might suppress *ccpp-1* defects. Polyglutamylases—enzymes that oppose deglutamylases—are known as TTL proteins [22, 23]. The *C. elegans* genome encodes six predicted TTL homologs

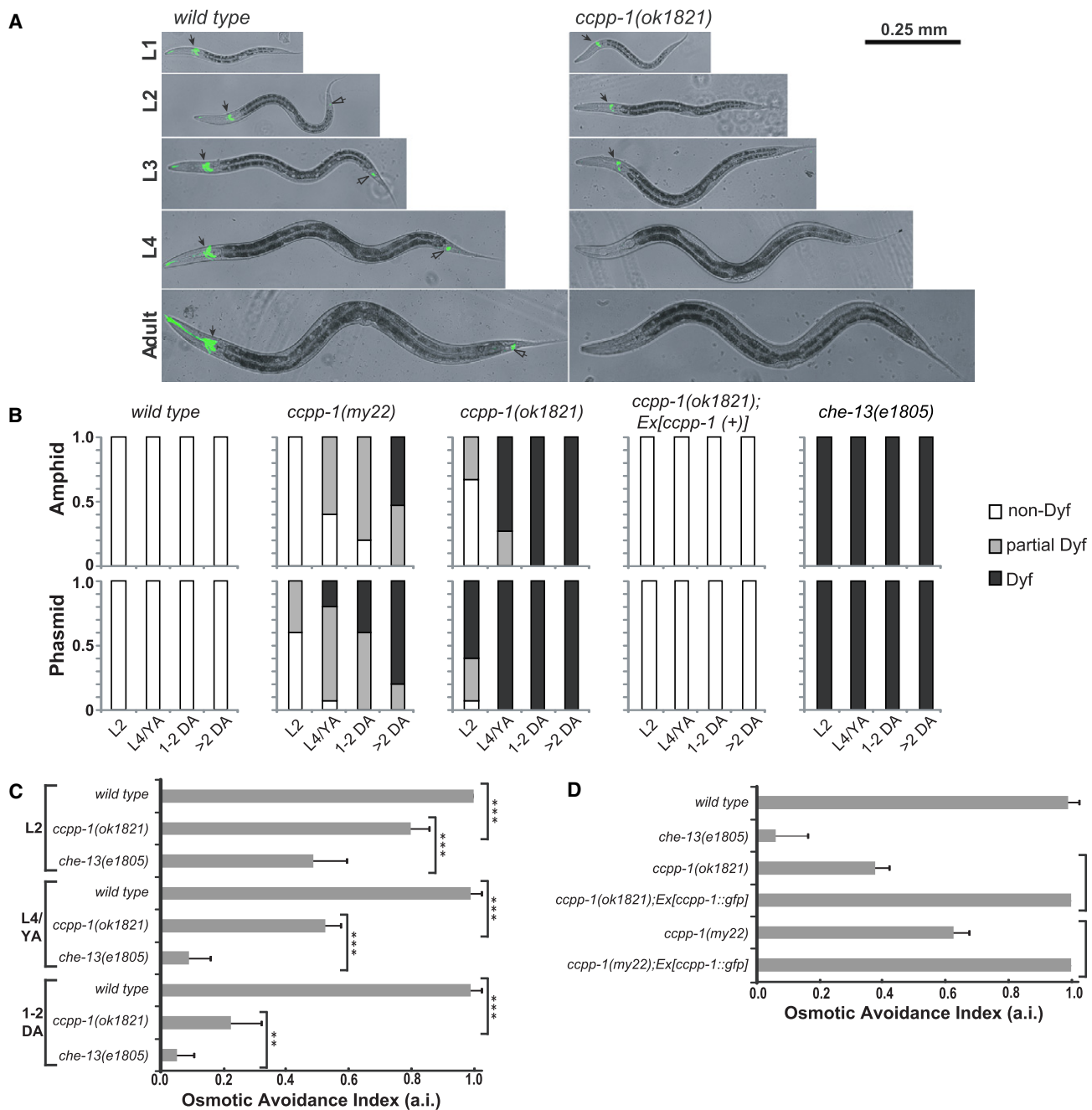


Figure 2. *ccpp-1* Mutants Exhibited Progressive Dyf and Osm Defects

(A) Amphid (solid arrows) and phasmid (hollow arrows) ciliated neurons of wild-type hermaphrodites were stained by Dil (pseudocolored green) at all developmental stages. *ccpp-1(ok1821)* amphid cilia in L1 larvae stained normally but became Dyf in later larval stages and adults.

(B) Dyf defects were scored in amphid and phasmid neurons in wild-type, *my22*, *ok1821*, and *che-13(e1805)* young adults (24 hr post-L4). Fifteen animals were scored for each indicated developmental stage and genotype.

(C) Wild-type animals exhibit osmotic avoidance behavior when challenged with an 8 M glycerol ring. Eighty hermaphrodites (eight trials, ten per trial) were tested for each stage/genotype. Osmotic avoidance index (a.i.) is the fraction of animals that avoided crossing the ring.

(D) The *ccpp-1* Osm defect was rescued by the *ccpp-1::gfp* transgene (eight trials, ten animals per trial tested). (Error bars indicate SEM; \*\*p = 0.0022 with Fisher's exact test; \*\*\*p < 0.0001 with Fisher's exact test).

[21]. In *C. elegans* core ciliated sensory neurons, *tll-4* mutants display drastically reduced antibody detection of polyglutamation signals in cilia, whereas *tll-9* mutants show a minor reduction [21]. IFT70/DYF-1 positively regulates polyglutamation in *C. elegans* and zebrafish [24]. To determine whether mutations in *tll-4*, *tll-9*, or *dyl-1* could suppress *ccpp-1* Cil

or Dyf phenotypes, we examined double-mutant combinations. Strikingly, *tll-4(tm3310)* suppressed the progressive Dyf, but not Cil, phenotype of *ccpp-1(ok1821)* mutants (Figures 4A and 4B; see also Figure S1 available online). *tll-9(tm3389)* did not suppress *ccpp-1* Cil or Dyf phenotypes (data not shown). Our results indicate that CcPP-1 opposes

**C. elegans Ccpp-1 Regulates Ciliary Stability**

5

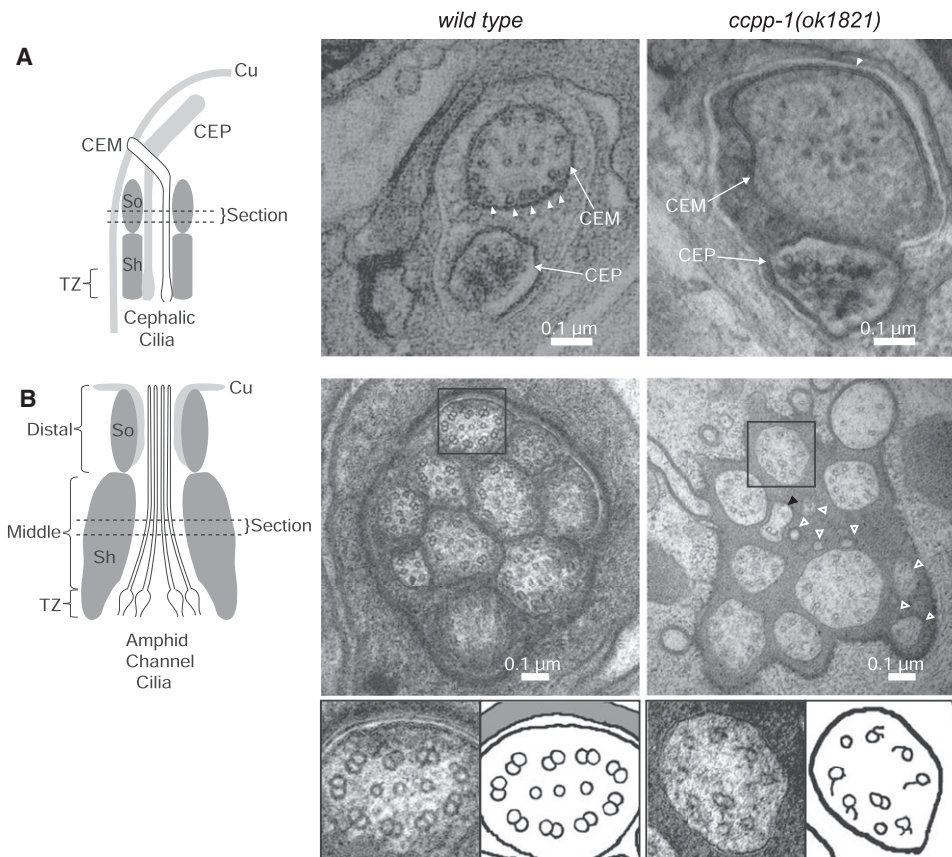


**Figure 3. *ccpp-1(ok1821)* Mutants Exhibit Ciliary Ultrastructure Defects**

Left diagrams show regions from which the cephalic (CEM and CEP) and amphid cilia images were taken. The following abbreviations are used: Cu, cuticle; Sh, sheath cell; So, socket cell; TZ, transition zone.

(A) Electron microscopy images of CEM and CEP cilia in wild-type and *ccpp-1(ok1821)* mutant adult males. Wild-type CEM cilia image (taken from a tomogram) contained many singlet microtubules (MTs) (19 singlets in section shown) closely apposed to the membrane (arrowheads). *ok1821* CEM cilia had fewer singlets (15 singlets in section shown), which were more distant from the membrane (arrowhead indicates one singlet near membrane). The *ok1821* CEM cilium diameter was larger than wild-type.

(B) Thin sections of amphid cilia in wild-type and *ccpp-1(ok1821)* adult males. Wild-type middle segments contain ten axonemes, each of which typically has nine outer doublets plus a variable number of inner singlets. The *ok1821* middle segment contained only eight intact axonemes plus what appear to be fragments of two cilia (hollow white arrowheads), one of which contains a singlet with attached broken B-tubule (black arrowhead). Most *ok1821* mutant axonemes had fewer MTs, with many doublets replaced by singlets or broken B-tubules. Bottom panels show boxed wild-type and mutant axonemes accompanied by cartoons. Refer to [Table 1](#) for quantification of images.

the activity of TLL-4 in polyglutamylation of proteins in amphid and phasmid cilia. Both the *dyf-1(mn335)* single mutant and *dyf-1(mn335) ccpp-1(my22)* double mutant were *Dyf* and *Cil* ([Figure S1](#)). Because *dyf-1* and *ccpp-1* single and double mutants display similar *Dyf* and *Cil* phenotypes, we cannot draw any conclusion about genetic interactions between them.

To detect polyglutamylation, we stained adult males with the monoclonal antibody GT335 [25]. In wild-type, GT335 neuronal staining was most apparent in the middle segments of amphid cilia, inner labial (IL) cilia in the nose, and phasmid cilia in the tail ([Figure 4C](#)). GT335 occasionally stained the CEM cilia in males, as visualized by PKD-2::GFP ([Figure 4D](#); [Figure S2A](#)). GT335 stained the distal tips of male tail ray neuronal cilia ([Figure 4C](#)). *ccpp-1* mutations had cell-type-specific effects on polyglutamylation. In general, GT335 immunofluorescence appeared to be more speckled in *ccpp-1* mutants ([Figure 4C](#)). *ccpp-1(my22)* and *ccpp-1(ok1821)* showed an approximately 5-fold increase over wild-type in the percent of CEM cilia with GT335 staining ([Figure 4D](#); [Figure S2A](#)). Increased polyglutamylation in *ccpp-1* CEM cilia is consistent with Ccpp-1

acting as a deglutamylase. Not surprisingly, the increased polyglutamylation in CEM cilia was not suppressed in *ccpp-1(ok1821);tll-4(tm3310)* or *dyf-1(mn335) ccpp-1(my22)* double mutants ([Figures S2A](#) and [S2B](#)).

In contrast, peak GT335 staining of amphid middle segments in *ccpp-1* adult males was significantly reduced to half or less of wild-type ([Figure 4E](#); [Figure S2C](#)). GT335 fluorescence in phasmid cilia of the tail and in male ray neuronal cilia also appeared to be decreased in *ccpp-1* mutants ([Figure 4C](#)). In some cases, ray neurons appeared to retain low polyglutamylation signals, but these signals were in ciliary bases rather than the tips of cilia ([Figure 4C](#), inset). The reduction of polyglutamylation in *ccpp-1* mutants was unexpected, but might reflect the ciliary ultrastructural defects in *ccpp-1* adults. In *ccpp-1(ok1821);tll-4(tm3310)* and *dyf-1(mn335) ccpp-1(my22)* double mutants, the reduction in polyglutamylation signals in amphid middle segments was similar to the *ccpp-1* single mutants ([Figure S2B](#) and [S2C](#)). Because both TLL-4 and DYF-1 positively regulate polyglutamylation, this result was expected.

Table 1. *ccpp-1* Mutants Display Cell-Specific Defects in Ciliary Ultrastructure

CEM Cilia	Wild-Type	<i>ccpp-1(ok1821)</i>
MT <sup>a</sup> singlets per cilium	20 ± 3	16 ± 4
cilium diameter (nm)	230 ± 40	384 ± 45
MT <sup>a</sup> displacement from membrane (nm)	25.1 ± 4.5	99 ± 15**
Amphid Channel Cilia		
cilia per amphid channel	10 ± 0	8.0 ± 1.4
cilia fragments	0 ± 0	3.5 ± 0.7
normal MT doublets per cilium	8.1 ± 0.9	2.0 ± 0.5**
central MT singlets	2.4 ± 0.3	0.5 ± 0.2**

We quantified characteristics of CEM cilia and amphid channel cilia middle segments (section is indicated in Figure 3) from transmission electron microscopy (TEM) cross-sections and tomographs. For CEM, n = 3 cilia per genotype; for amphids, n = 4 amphid channels; and for wild type, n = 2 amphid channels for *ok1821*. For number of doublets, 25 wild-type and eight *ok1821* cilia had sufficient resolution in TEM or tomograph images to determine the number of normal doublets and number of singlets; values are average ± standard deviation (\*\*p < 0.01 by Mann-Whitney test).

<sup>a</sup>MT, microtubule.

To determine whether *ccpp-1* mutations perturbed other PTMs, we examined polyglycylated tubulin and Δ2-tubulin by antibody staining. The *C. elegans* genome lacks predicted polyglycylating enzymes [21]; as expected, we detected no polyglycylation signals (data not shown). An anti-Δ2-tubulin polyclonal antibody stained pairs of lateral neurites in wild-type males but did not stain cilia except the phasmids in the tail (Figure S2D). In *ccpp-1* mutants, the anti-Δ2-tubulin antibody also dimly stained some cilia in the nose (Figure S2D).

### CCPP-1 Regulates the Kinesin-3 KLP-6 and the Kinesin-2 OSM-3

To determine whether *ccpp-1* regulates the abundance or localization of ciliary motor proteins, we examined KLP-6, OSM-3/KIF17, and the kinesin-II cargo OSM-6. In wild-type, KLP-6::GFP is diffusely localized throughout neuronal cell bodies, axons, dendrites, and cilia of the male-specific CEM, HOB, and RnB neurons and the core IL2 neurons (Figure 5A) [26]. In *ccpp-1(my22)* mutants, KLP-6::GFP accumulated in cilia (Figure 5A). We used the *pkd-2* promoter to drive expression of *ccpp-1* in the male-specific CEM, HOB, and RnB neurons [27], which rescued KLP-6::GFP abundance and localization in cilia of these neurons (Figures 5B and 5C). We conclude that CCPP-1 acts cell autonomously to regulate the distribution of KLP-6 and its putative cargo, PKD-2.

Next, we investigated OSM-3 in CEM cilia for two reasons: first, we could observe the effects of *ccpp-1(ok1821)* on OSM-3::GFP motility and localization in a single cilium, whereas the amphid channel contains cilia of eight different neuronal types [19]. Second, TEM experiments indicated that amphid cilia in *ccpp-1* mutants had variable structural defects (Figure 3), indicating that individual amphid channel cilia might be affected differently or with different time courses. In CEM cilia, the majority of OSM-3 moves independently of kinesin-II and IFT complexes [4]. The localization of OSM-3::GFP was similar in wild-type and *ccpp-1(ok1821)* CEM cilia (Figure 6A). However, the apparent velocity of motile OSM-3::GFP puncta in CEM cilia was significantly increased in *ccpp-1(ok1821)* mutants ( $1.07 \pm 0.07 \mu\text{m/s}$  versus  $0.75 \pm 0.03 \mu\text{m/s}$ ; Figure 6B). Mutation of *ttil-4* had no effect on OSM-3::GFP localization or velocity in either wild-type or *ccpp-1* backgrounds

(Figures S3A–S3C), consistent with the failure of *ttil-4* to suppress the Cil phenotype of *ccpp-1*.

OSM-6 is an IFT-B polypeptide that is transported solely by kinesin-II in CEM cilia [4]. *ccpp-1(ok1821)* did not affect abundance, localization, or velocity of OSM-6::GFP (Figures 6C and 6D; Figure S3D). We conclude that, in CEM cilia, CCPP-1 regulates the accessory motors OSM-3 and KLP-6 but does not regulate the canonical IFT motor, heterotrimeric kinesin-II.

## Discussion

### Loss of CCPP-1 Function Causes Ciliary Transport Defects and Progressive Deterioration of Ciliary Structure and Function

Here we show that the *C. elegans* carboxypeptidase CCPP-1 plays critical cell-specific roles in maintaining ciliary integrity and function in vivo. *ccpp-1* mutants are defective in localization and abundance of the kinesin-3 KLP-6 and its putative cargo PKD-2 in male-specific sensory cilia. Mutant males also have a corresponding mating defect in response behavior, which requires PKD-2 and KLP-6 function [14, 26]. Unlike IFT mutants, *ccpp-1* mutant larvae exhibit amphid cilia that fill with dye and support osmotic avoidance behavior. However, *ccpp-1* mutants display a progressive, age-dependent dye-filling defect of cilia in amphid and phasmid sensory neurons, which correlates with deficits in osmotic avoidance behavior. We propose that CCPP-1 is needed for ciliary maintenance rather than ciliogenesis. Two previous studies have shown that CCP1 requires a functional carboxypeptidase domain to rescue defects in *pcd* mice [28, 29]. The *ccpp-1(my22)* mutation, which encodes a G596R substitution, demonstrates that the FESGNL motif is also essential for full function (Figure 1B). However, the function of this domain, or indeed, the CCPP-1 protein itself, is not fully understood.

### CCPP-1 Regulation of the Tubulin Code Affects Specific Kinesin Motors

Our results are consistent with a proposed “tubulin code” model, in which PTMs provide signposts that regulate the localization or activity of motors [5–8]. In male-specific CEM cilia of *ccpp-1* mutants, ciliary localization of KLP-6 is elevated and the apparent velocity of OSM-3::GFP is increased. In contrast, the localization and motility of the kinesin-II-driven IFT-B polypeptide OSM-6::GFP are unaffected. We propose that CCPP-1-mediated MT modification normally regulates KLP-6 subcellular distribution and OSM-3 velocity in CEM cilia. Identification of additional roles for CCPP-1, such as regulating dynein-based transport, motor recycling, or cargo-motor binding, await future studies.

### CCPP-1 Regulates MT Polyglutamylation, MT Stability, and Ciliary Stability

In CEM cilia, CCPP-1 regulates polyglutamylation levels independently of TTLL-4 (Figure 4; Figures S1, S2A, S2B, S3C). We suggest that polyglutamylation in CEM cilia is normally maintained at a low level by CCPP-1 and an unknown TTLL polyglutamylase. Because misregulation of MT polyglutamylation affects the kinesin-2 OSM-3 and the kinesin-3 KLP-6, we propose that the PKD-2::GFP Cil phenotype could be secondary to motor function defects. Our data strongly suggest that CCPP-1 reduces polyglutamylation of MTs and opposes polyglutamylating enzymes in *C. elegans* cilia.

**C. elegans CCPP-1 Regulates Ciliary Stability**

7

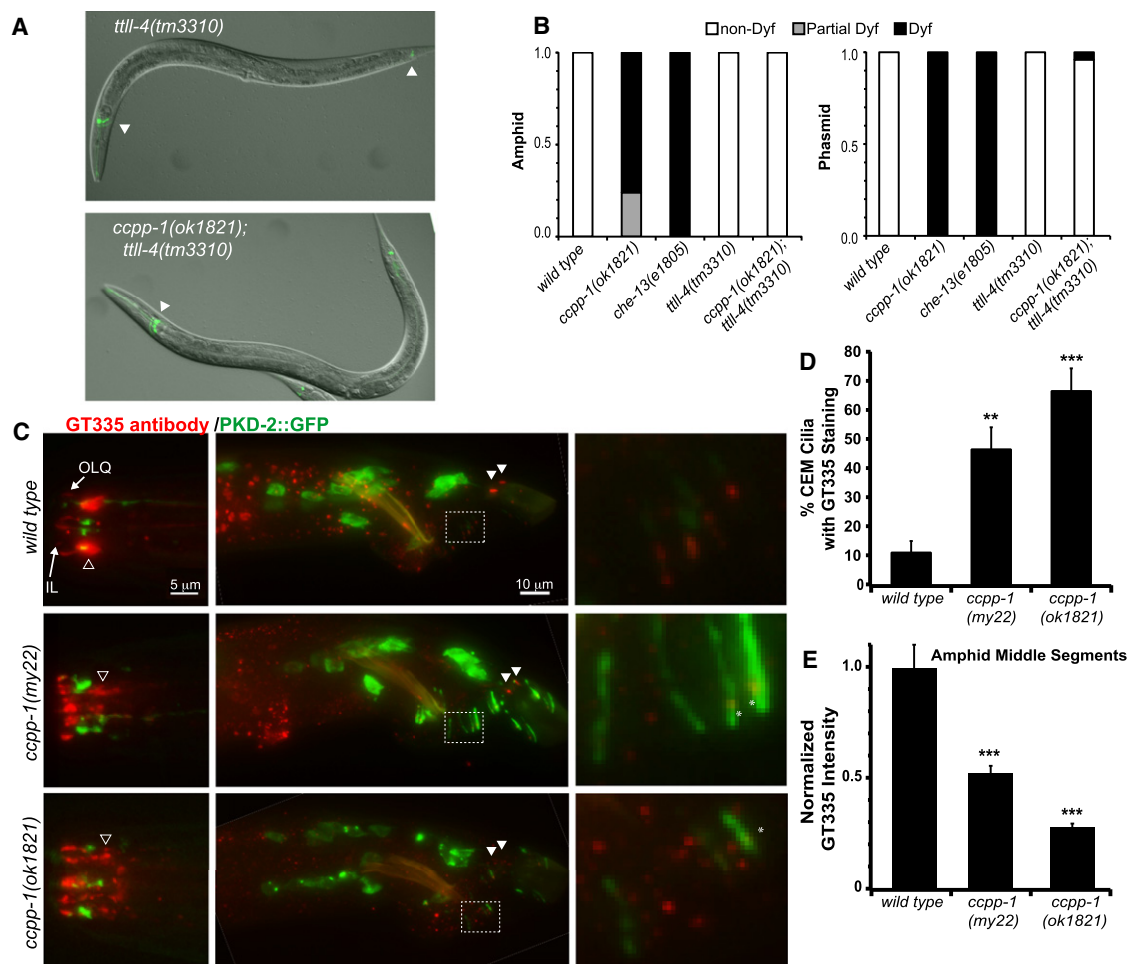


**Figure 4. Loss of CCPP-1 Results in Altered Polyglutamylation of Sensory Cilia**

(A) Dye uptake (pseudocolored green) was normal in young adult hermaphrodite *tll-4(tm3310)* mutants (left), which were previously reported to lack polyglutamylation in cilia [21]. Deletion of *tll-4* suppressed the Dyf phenotype of *ccpp-1* (right). Arrowheads indicate dye-filled amphid and phasmid neurons. (B) Penetrance of Dyf defects in amphid and phasmid neurons. Fifty young adult hermaphrodites per genotype were tested. (C) Staining of wild-type and *ccpp-1* mutant young adult males with GT335, a monoclonal antibody that detects polyglutamylation, most prominently in amphid middle segments (hollow arrowhead). An IL and putative outer labial quadrant cilium are indicated in the nose. GT335 rarely stained wild-type CEM cilia, which express PKD-2::GFP. In the tail, phasmid cilia (solid arrowheads) were brightly stained. Right, enlarged boxed area containing several ray neuron dendrites and cilia. Asterisks mark polyglutamylation signals that are abnormally localized to the ciliary base in *ccpp-1* mutants. (D) *ccpp-1* mutations increased the incidence of GT335 staining of CEM cilia, which were identified by PKD-2::GFP (\*\* $p < 0.01$ ; \*\*\* $p < 0.001$  versus wild-type, ANOVA/Tukey test;  $n = 19$ –22 males per genotype; scored blindly). (E) The normalized peak pixel value of GT335 staining in the area containing amphid middle segments was significantly lower in mutants (error bars indicate SEM; \*\*\* $p < 10^{-5}$  versus wild-type, by ANOVA/Tukey HSD test;  $n = 10$  males per genotype). See also Figure S2.

Our results also predict that CCPP-1 activity depends on cell-specific factors, because loss of TLL-4 suppresses *ccpp-1* Dyf, but not Cil, defects. Such cell-specific factors may include particular tubulin isoforms or regulators of PTMs. In amphid cilia, mutation of *ccpp-1* decreases polyglutamylation levels (Figure 4; Figure S2C)—counter to our expectation, considering that mammalian CCP1 deglutamylates MTs and that loss of the polyglutamylase TLL-4 suppressed the Dyf phenotype of *ccpp-1* mutants. However, hyperglutamylation destabilizes axonemal MTs in *Tetrahymena* [30]. Degradation of extensively polyglutamylated MTs, as well as the loss of some amphid cilia, might explain the paradoxical loss of GT335 staining in amphid cilia middle segments in *ccpp-1* adults.

Our ultrastructural studies support this hypothesis (Figure 3B; Table 1). In *ccpp-1* amphid cilia, the number of both

doublets and singlets is reduced by 75% compared to wild-type (Table 1). In *Chlamydomonas* ciliary MT doublets, B-tubules are the main site of polyglutamylation [31]. Assuming this is true in *C. elegans*, the B-tubule defects we observed are likely to explain the reduction of GT335 staining in *ccpp-1* amphid cilia. These ultrastructural defects are also consistent with the progressive Dyf phenotype in *ccpp-1* mutants. We propose that the degree of polyglutamylation must be tightly controlled for MT doublet stability.

**Does Mutation of CCP1 in Mammals Cause Ciliopathic Neurodegeneration?**

A greater understanding of the function of CCPP-1 is of interest because the mammalian homolog, CCP1, is required for survival of several populations of neurons in the mouse brain [12, 13]. In addition to adult-onset degeneration of

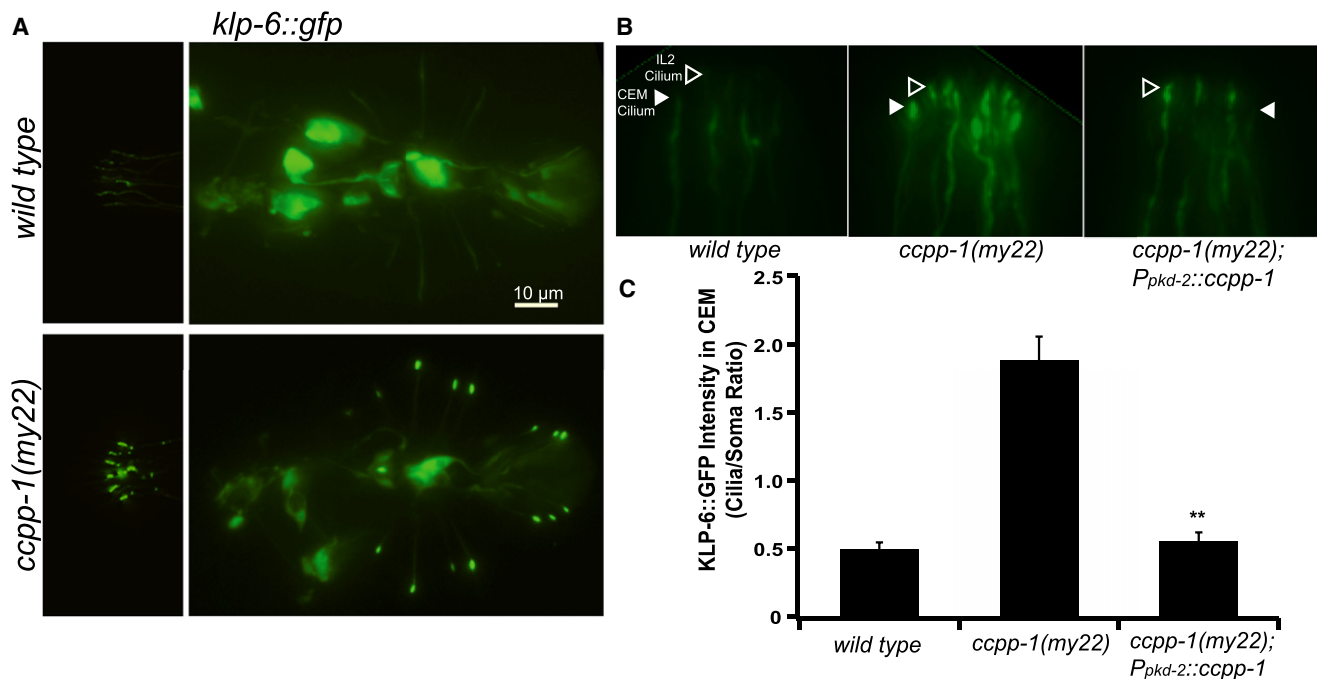


**Figure 5. CCP-1 Is Needed for Proper Localization of KLP-6::GFP in IL2 and Male-Specific Neurons**

(A) KLP-6::GFP localization in IL2 and CEM neurons (left) and in HOB and RnB neurons in the tail (right) is diffuse in wild-type males. In contrast, KLP-6::GFP is highly enriched in cilia in *ccpp-1(my22)* mutants. (B) A magnified view of IL2 (hollow arrowheads) and CEM (solid arrowheads) cilia containing KLP-6::GFP in wild-type, *ccpp-1(my22)*, and *ccpp-1(my22)* rescued young adult males. (C) Quantification of KLP-6::GFP localization (ratio of ciliary to somatic fluorescence) in CEM neurons. KLP-6::GFP localization defects in *ccpp-1(my22)* mutant cilia were rescued by *P<sub>pkd-2</sub>::ccpp-1* in male-specific CEM (and RnB, data not shown) neurons (error bars indicate SEM; n = 9 or 10 animals per genotype; \*\*p < 0.01 by t test versus *ccpp-1(my22)*).

cerebellar Purkinje neurons and sperm immotility, other defects, such as degeneration of retinal photoreceptors, olfactory bulb mitral neurons, and thalamic neurons, result from loss of CCP1 [12, 13]. All of the cell types affected in *pcd* mice are ciliated or flagellated. RNAi-mediated knockdown of CCP1 reduced ciliary length in cultured human cells [32]. We show here, for the first time, that CCP-1 is required for maintenance of the structure and function of cilia in *C. elegans*.

Consequently, we propose that neurodegeneration and other defects in *pcd* mice could be caused by ciliopathy. Vertebrate primary cilia may be specialized for intercellular signaling such as Wnt and Hedgehog (reviewed in [33]). In addition to developmental roles, such signaling might be needed for cellular survival and maintenance of cilia in which receptors reside. Hence, further study of *ccpp-1*, tubulin posttranslational modification, and ciliary dynamics in *C. elegans* should provide more insight on ciliopathic degenerative diseases.

#### Experimental Procedures

##### Strains Used

The genotypes of all strains used are described in [Supplemental Experimental Procedures](#).

##### PKD-2::GFP Localization

Strains used were as follows: PT443, PT1645, PT1931, PT1932, PT2168, PT2169, PT2170, PT2171, PT2172, PT2379, and PT2381.

We isolated L4 males from hermaphrodites 20–24 hr before observation. To score the Cil phenotype, we observed PKD-2::GFP localization on the Zeiss Axioplan2 microscope using the 10× objective. At this magnification, GFP fluorescence was not visible anywhere outside of the cell bodies of the CEM, RnB, or HOB neurons in wild-type males. In *ccpp-1* mutants,

PKD-2::GFP was visible in dendrites and cilia, especially in rays. Images of PKD-2::GFP localization were captured using 63× or 100× objectives.

##### Antibody Staining

Strains used were as follows: PT443, PT1645, PT2168, PT2171, PT2172, PT2379, and PT2381.

Gravid adults were bleached to obtain age-synchronized embryos, which were then fixed as 1-day-old adults. We used the fixation and staining method described in [34]. Fixed worms were stored at 4°C for up to 1 month before antibody staining. Animals were stained overnight at room temperature with a 1:600 dilution in antibody buffer A of GT335 (a monoclonal antibody which binds the branch point of both monoglutamylated and polyglutamylated substrates [25]), 1:500 dilution of AB3203 (polyclonal antibody that binds  $\Delta 2$ -tubulin; Millipore [35]), 1:200 dilution of TAP952 (monoclonal antibody that binds both monoglycylated and polyglycylated tubulin, a gift from the Drummond laboratory), and a 1:200 dilution of R2302 anti-poly-G (rabbit polyclonal antibody that binds polyglycylated tubulin, a gift from the Gorovsky laboratory). Alexa Fluor 578-conjugated anti-mouse or anti-rabbit secondary antibodies (Invitrogen) were used at a dilution of 1:2,000 and incubated for 2 hr at room temp with gentle agitation. See [Supplemental Experimental Procedures](#) for details.

##### Statistical Methods

All data values are expressed as mean  $\pm$  standard error unless indicated. To determine the statistical significance of differences in experimental results, we conducted statistical tests in IGOR 6 (Wavemetrics, Inc.), Statplus (Analystsoft), or Prism (Graphpad Software).

##### Other Methods

See [Supplemental Experimental Procedures](#) for *C. elegans* culture, mapping of *my22* mutation, transgenesis, microscopy, KLP-6::GFP localization, OSM-3::GFP and OSM-6::GFP motility, male mating response behavior, dye-filling and osmotic avoidance behavior, and electron microscopy and tomography.

**C. elegans Ccpp-1 Regulates Ciliary Stability**

9

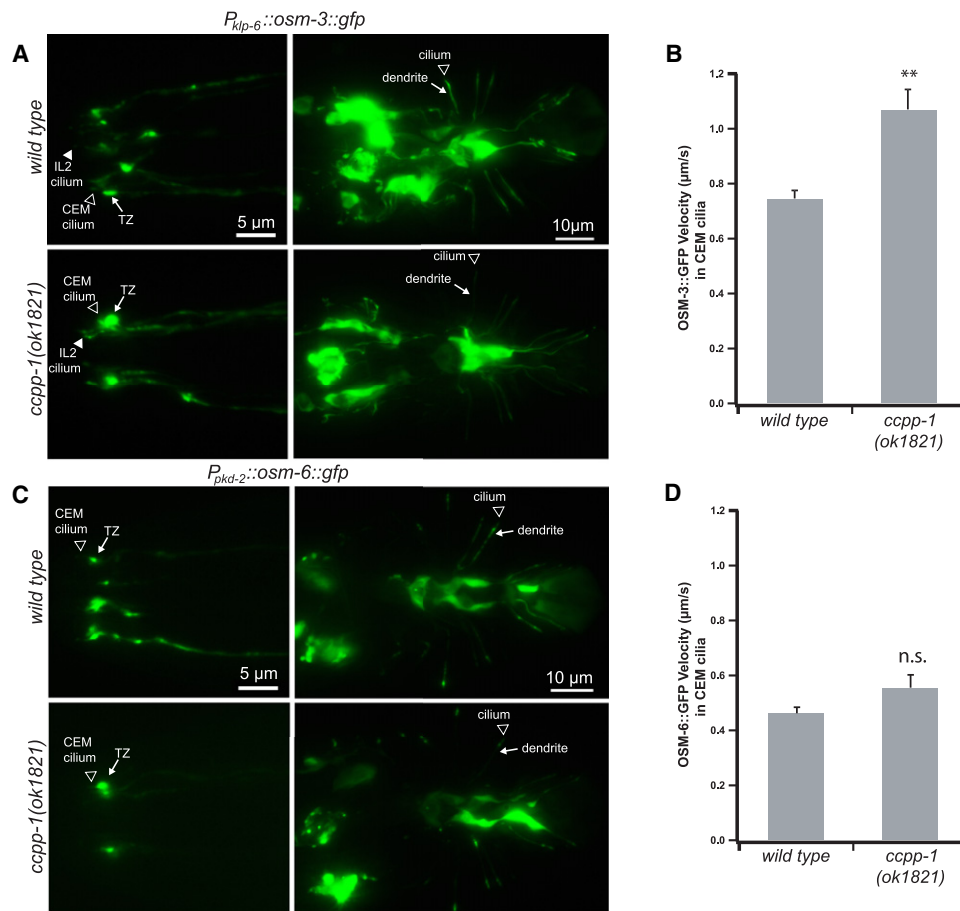


**Figure 6. Ccpp-1 Regulates the Velocity of OSM-3::GFP but Not Kinesin-II-Driven IFT-B Polypeptide OSM-6::GFP in CEM Cilia**

(A) In wild-type and *ccpp-1(ok1821)* young adult males, *k1p-6* promoter-driven OSM-3::GFP was visible diffusely in cell bodies, dendrites, and cilia, with some accumulation in transition zones (TZ). (B) OSM-3::GFP particles moved faster in *ccpp-1* CEM cilia (78 particles in seven wild-type males; 81 particles in ten *ccpp-1(ok1821)* males; \*\* $p < 10^{-4}$  by ANOVA/Tukey test). (C and D) OSM-6::GFP localization and velocity in CEM cilia was similar in wild-type and *ok1821* males (error bars indicate SEM; 55 particles in six wild-type males; 61 particles in seven *ccpp-1(ok1821)* males; ns indicates no significant difference). See also [Figure S3](#).

**Supplemental Information**

Supplemental Information includes three figures and Supplemental Experimental Procedures and can be found with this article online at [doi:10.1016/j.cub.2011.08.049](https://doi.org/10.1016/j.cub.2011.08.049).

**Acknowledgments**

This work was supported by the National Institutes of Health (NIH) NRSA 5F32NS56540-4 and NJCSCR 10-2951-SCR-E-0 fellowships to R.O.; a Fulbright Fellowship and a Lars Hiertas Minne Foundation grant to B.P.P.; NIH RO1DK059418 grant to M.M.B.; grants from the Swedish Research Council, Marcus Borgström Foundation, and the NordForsk Nordic Networks for *C. elegans* and Cilia and Centrosome Research to P.S.; NIH RR12596 grant to D.H.H.; and Einstein funds for access to the New York Structural Biology Center (NYSBC). We thank Bill Rice and KD Derr (NYSBC) for help in using the Technai20 microscope and creating electron tomograms. Some nematode strains used in this work were provided by the *Caenorhabditis* Genetics Center, which is funded by the NIH National Center for Research Resources, The *C. elegans* Gene Knockout Consortium, and the National Bioresource Project for the Nematode (Japan). Thanks to the Drummond and Gorovsky laboratories for the anti-polyglycylation antibodies. We also thank Natalia Morsci, Andrew Jauregui, and Julie Maguire for plasmids and strains and members of the Barr laboratory for discussions and constructive criticism of this manuscript.

Received: February 28, 2011

Revised: August 1, 2011

Accepted: August 19, 2011

Published online: October 6, 2011

**References**

1. Fliegauf, M., Benzing, T., and Omran, H. (2007). When cilia go bad: cilia defects and ciliopathies. *Nat. Rev. Mol. Cell Biol.* 8, 880–893.
2. Scholey, J.M. (2008). Intraflagellar transport motors in cilia: moving along the cell's antenna. *J. Cell Biol.* 180, 23–29.
3. Pan, X., Ou, G., Civelekoglu-Scholey, G., Blacque, O.E., Endres, N.F., Tao, L., Mogilner, A., Leroux, M.R., Vale, R.D., and Scholey, J.M. (2006). Mechanism of transport of IFT particles in *C. elegans* cilia by the concerted action of kinesin-II and OSM-3 motors. *J. Cell Biol.* 174, 1035–1045.
4. Morsci, N.S., and Barr, M.M. (2011). Kinesin-3 KLP-6 regulates intraflagellar transport in male-specific cilia of *Caenorhabditis elegans*. *Curr. Biol.* 21, 1239–1244.
5. Bulinski, J.C., and Gundersen, G.G. (1991). Stabilization of post-translational modification of microtubules during cellular morphogenesis. *Bioessays* 13, 285–293.
6. Verhey, K.J., and Gaertig, J. (2007). The tubulin code. *Cell Cycle* 6, 2152–2160.

7. Janke, C., and Kneussel, M. (2010). Tubulin post-translational modifications: encoding functions on the neuronal microtubule cytoskeleton. *Trends Neurosci.* **33**, 362–372.
8. Ikegami, K., and Setou, M. (2010). Unique post-translational modifications in specialized microtubule architecture. *Cell Struct. Funct.* **35**, 15–22.
9. Ikegami, K., Heier, R.L., Taruishi, M., Takagi, H., Mukai, M., Shimma, S., Taira, S., Hatanaka, K., Morone, N., Yao, I., et al. (2007). Loss of alpha-tubulin polyglutamylation in ROSA22 mice is associated with abnormal targeting of KIF1A and modulated synaptic function. *Proc. Natl. Acad. Sci. USA* **104**, 3213–3218.
10. Bae, Y.K., Lyman-Gingerich, J., Barr, M.M., and Knobel, K.M. (2008). Identification of genes involved in the ciliary trafficking of *C. elegans* PKD-2. *Dev. Dyn.* **237**, 2021–2029.
11. Rogowski, K., van Dijk, J., Magiera, M.M., Bosc, C., Deloulme, J.C., Bossou, A., Peris, L., Gold, N.D., Lacroix, B., Grau, M.B., et al. (2010). A family of protein-deglutamylating enzymes associated with neurodegeneration. *Cell* **143**, 564–578.
12. Fernandez-Gonzalez, A., La Spada, A.R., Treadaway, J., Higdon, J.C., Harris, B.S., Sidman, R.L., Morgan, J.I., and Zuo, J. (2002). Purkinje cell degeneration (*pccd*) phenotypes caused by mutations in the axotomy-induced gene, *Nna1*. *Science* **295**, 1904–1906.
13. Mullen, R.J., Eicher, E.M., and Sidman, R.L. (1976). Purkinje cell degeneration, a new neurological mutation in the mouse. *Proc. Natl. Acad. Sci. USA* **73**, 208–212.
14. Barr, M.M., DeModena, J., Braun, D., Nguyen, C.Q., Hall, D.H., and Sternberg, P.W. (2001). The *Caenorhabditis elegans* autosomal dominant polycystic kidney disease gene homologs *lov-1* and *pkd-2* act in the same pathway. *Curr. Biol.* **11**, 1341–1346.
15. Altschul, S.F., Gish, W., Miller, W., Myers, E.W., and Lipman, D.J. (1990). Basic local alignment search tool. *J. Mol. Biol.* **215**, 403–410.
16. Rodriguez de la Vega, M., Sevilla, R.G., Hermoso, A., Lorenzo, J., Tanco, S., Diez, A., Fricker, L.D., Bautista, J.M., and Avilés, F.X. (2007). Nna1-like proteins are active metallocarboxypeptidases of a new and diverse M14 subfamily. *FASEB J.* **21**, 851–865.
17. Liu, K.S., and Sternberg, P.W. (1995). Sensory regulation of male mating behavior in *Caenorhabditis elegans*. *Neuron* **14**, 79–89.
18. Barrios, A., Nurrish, S., and Emmons, S.W. (2008). Sensory regulation of *C. elegans* male mate-searching behavior. *Curr. Biol.* **18**, 1865–1871.
19. Perkins, L.A., Hedgecock, E.M., Thomson, J.N., and Culotti, J.G. (1986). Mutant sensory cilia in the nematode *Caenorhabditis elegans*. *Dev. Biol.* **117**, 456–487.
20. Culotti, J.G., and Russell, R.L. (1978). Osmotic avoidance defective mutants of the nematode *Caenorhabditis elegans*. *Genetics* **90**, 243–256.
21. Kimura, Y., Kurabe, N., Ikegami, K., Tsutsumi, K., Konishi, Y., Kaplan, O.I., Kunitomo, H., Iino, Y., Blacque, O.E., and Setou, M. (2010). Identification of tubulin deglutamylase among *Caenorhabditis elegans* and mammalian cytosolic carboxypeptidases (CCPs). *J. Biol. Chem.* **285**, 22936–22941.
22. Janke, C., Rogowski, K., Wloga, D., Regnard, C., Kajava, A.V., Strub, J.M., Temurak, N., van Dijk, J., Boucher, D., van Dorsselaer, A., et al. (2005). Tubulin polyglutamylase enzymes are members of the TTL domain protein family. *Science* **308**, 1758–1762.
23. Ikegami, K., Mukai, M., Tsuchida, J., Heier, R.L., Macgregor, G.R., and Setou, M. (2006). TTL7 is a mammalian beta-tubulin polyglutamylase required for growth of MAP2-positive neurites. *J. Biol. Chem.* **281**, 30707–30716.
24. Pathak, N., Obara, T., Mangos, S., Liu, Y., and Drummond, I.A. (2007). The zebrafish *fleer* gene encodes an essential regulator of cilia tubulin polyglutamylation. *Mol. Biol. Cell* **18**, 4353–4364.
25. Wolff, A., de Néchaud, B., Chillet, D., Mazarguil, H., Desbruyères, E., Audebert, S., Eddé, B., Gros, F., and Denoulet, P. (1992). Distribution of glutamylated alpha and beta-tubulin in mouse tissues using a specific monoclonal antibody, GT335. *Eur. J. Cell Biol.* **59**, 425–432.
26. Peden, E.M., and Barr, M.M. (2005). The KLP-6 kinesin is required for male mating behaviors and polycystin localization in *Caenorhabditis elegans*. *Curr. Biol.* **15**, 394–404.
27. Barr, M.M., and Sternberg, P.W. (1999). A polycystic kidney-disease gene homologue required for male mating behaviour in *C. elegans*. *Nature* **401**, 386–389.
28. Wang, T., Parris, J., Li, L., and Morgan, J.I. (2006). The carboxypeptidase-like substrate-binding site in *Nna1* is essential for the rescue of the Purkinje cell degeneration (*pccd*) phenotype. *Mol. Cell. Neurosci.* **33**, 200–213.
29. Chakrabarti, L., Eng, J., Martinez, R.A., Jackson, S., Huang, J., Possin, D.E., Sopher, B.L., and La Spada, A.R. (2008). The zinc-binding domain of *Nna1* is required to prevent retinal photoreceptor loss and cerebellar ataxia in Purkinje cell degeneration (*pccd*) mice. *Vision Res.* **48**, 1999–2005.
30. Wloga, D., Dave, D., Meagley, J., Rogowski, K., Jerka-Dziadosz, M., and Gaertig, J. (2010). Hyperglutamylated tubulin can either stabilize or destabilize microtubules in the same cell. *Eukaryot. Cell* **9**, 184–193.
31. Kubo, T., Yanagisawa, H.A., Yagi, T., Hirono, M., and Kamiya, R. (2010). Tubulin polyglutamylase regulates axonemal motility by modulating activities of inner-arm dyneins. *Curr. Biol.* **20**, 441–445.
32. Kim, J., Lee, J.E., Heynen-Genel, S., Suyama, E., Ono, K., Lee, K., Ideker, T., Aza-Blanc, P., and Gleeson, J.G. (2010). Functional genomic screen for modulators of ciliogenesis and cilium length. *Nature* **464**, 1048–1051.
33. Gerdes, J.M., Davis, E.E., and Katsanis, N. (2009). The vertebrate primary cilium in development, homeostasis, and disease. *Cell* **137**, 32–45.
34. Lewis, J.A., and Fleming, J.T. (1995). Basic culture methods. *Methods Cell Biol.* **48**, 3–29.
35. Paturle-Lafanechère, L., Eddé, B., Denoulet, P., Van Dorsselaer, A., Mazarguil, H., Le Caer, J.P., Wehland, J., and Job, D. (1991). Characterization of a major brain tubulin variant which cannot be tyrosinated. *Biochemistry* **30**, 10523–10528.
36. Kosugi, S., Hasebe, M., Tomita, M., and Yanagawa, H. (2009). Systematic identification of cell cycle-dependent yeast nucleocytoplasmic shuttling proteins by prediction of composite motifs. *Proc. Natl. Acad. Sci. USA* **106**, 10171–10176.
37. de Castro, E., Sigrist, C.J., Gattiker, A., Bulliard, V., Langendijk-Genevaux, P.S., Gasteiger, E., Bairoch, A., and Hulo, N. (2006). ScanProsite: detection of PROSITE signature matches and ProRule-associated functional and structural residues in proteins. *Nucleic Acids Res.* **34** (Web Server issue), W362–W365.